High-nuclearity Metal-Cyanide Cluster[Mo6Cu14] with Photomagnetic Properties

Nathalie Bridonneau[a], Lise-Marie Chamoreau[a], GoeffreyGontard[a], Jean-Louis Cantin,[b]JurgenvonBardeleben,[b] andValérie Marvaud[a]*.

Supplementary Information

[Mo$_6$(Cu-tacn)$_{14}$], noted (1)

[Mo$_3$(Cu-Me$_3$tacn)$_4$], noted (2)
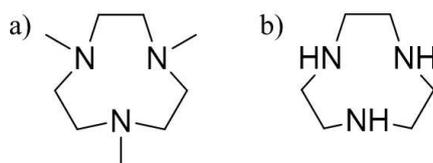
1. Experimental Section

Figure S1:*Ligands used: a) Me₃tacn (1,4,7-trimethyl-1,4,7-triazacyclo-nonane) and b) tacn (1,4,7-triazacyclononane).*
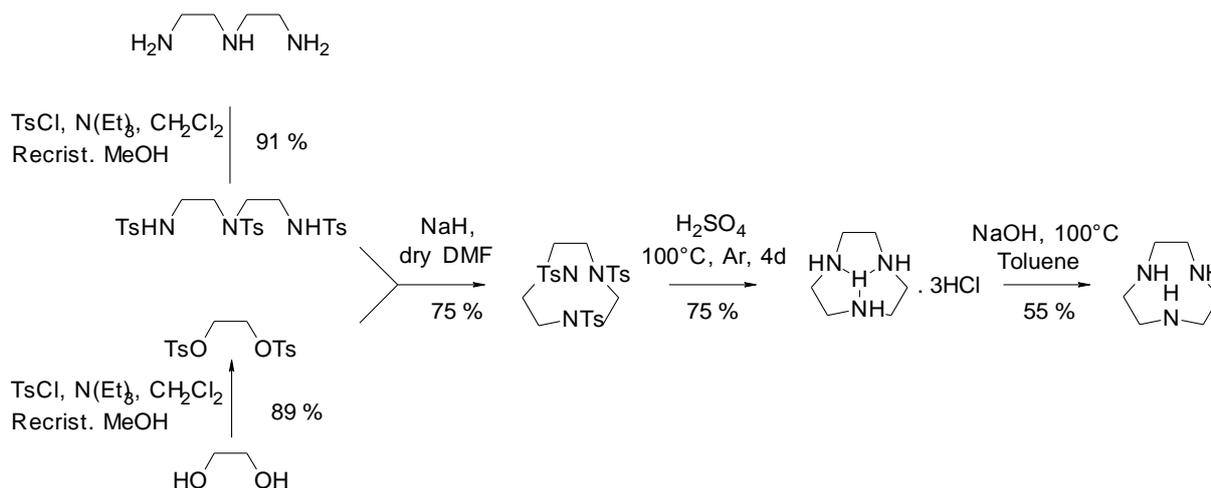

Figure S2:*Synthesis of tacn(1,4,7-triazacyclononane)ligand*

Tacn ligand was obtained from the condensation of the tosylateddiethylenetriamine and ethylene glycol in presence of NaH. Removal of the tosyl groups was achieved under acidic conditions at 100°C for four days. Addition of NaOH enabled to get the cyclic triamine.

Ditosyl ethylene glycol. Tosyl chloride (55 g, 0.29 mol, 2.24 eq) and triethylamine (29 g, 0.29 mol, 2.24 eq) were dissolved in 200 mL of dichloromethane over an ice bath and the solution was stirred for 10 min. Ethylene glycol (8 g, 0.129 mol, 1 eq) was then added dropwise to the solution for 30 min and the reaction was stirred overnight. The reaction mixture was divided in four portions and poured into 300 mL of water before being extracted 3 times with 50 mL of dichloromethane. The organic layer was dried with $MgSO_4$ and filtered. After evaporation of the solvent the orange powder was rinsed with methanol to produce 40.2 g of a white powder in an 85 % yield.

RMN ^{1}H (300 MHz, CDCl₃): δ 7.73 (d, 4H, CH aromatic, J= 9 Hz), 7.34 (d, 4H, CH aromatic, J= 9 Hz), 4.18 (s, 4H, CH₂), 2.45 (s, 6H, CH₃).

Tritosyldiethylenetriamine. Tosyl chloride (46 g, 0.24 mol, 3.1 eq) and triethylamine (25.2 g, 0.25 mol, 3.2 eq) were dissolved in 200 mL of dichloromethane over an ice bath and the solution was stirred for 10 min. Diethylenetriamine (8 g, 0.078 mol, 1 eq) was then added dropwise to the solution and the reaction was stirred overnight. Evaporation of the solvent

followed by recrystallization in methanol gave a white powder in a 91 % yield. NMR ^{1}H (300 MHz, acetone-d6) : δ 7,72 (d, 4H, CH aromatic, J= 9 Hz), 7,61 (d, 2H, CH aromatic, J= 9 Hz), 7,36 (m, 6H, CH aromatic), 6,51 (s, 1H, NH), 3,16 (m, 4H, CH_2), 3,02 (m, 4H, CH_2), 2,40 (s, 9H, CH_3).

1,4,7-Triazacyclononane Tritosylate. To a solution of tritosyldiethylenetriamine (24 g, 0.042 mol, 1 eq) in 150 mL of dried DMF at 100 °C were added 6 g of NaH (60% in oil, 0.25 mol) in 500 mg portions (!careful, H_2 production). Ditosyl ethylene glycol (15.7 g, 0.042 mol, 1 eq) in 150 mL of dried DMF were then added dropwise and the solution turned brown. The reaction mixture was heated for 3 more hours before being poured over 1 L of degassed water at 0°C. The resulting mixture was vigorously stirred for 15 hours then filtered and washed with water then dried with ethanol and ether, producing 19 g of a light brown solid in a 75 % yield. NMR ^{1}H (300 MHz, $CDCl_3$) :δ 7.72 (d, 6H, CH aromatic, J= 9 Hz), 7.33 (d, 6H, CH aromatic, J= 9 Hz), 3.41 (s, 12H, CH_2), 2.43 (s, 9H, CH_3).

1,4,7-Triazacyclononane · Trihydrochlorate (TACN · 3 HCl). 1,4,7-Triazacyclononane tritosylate (19 g, 0.032 mol) in 40 mL of concentrated H_2SO_4 was heated at 100°C for 4 days under an argon atmosphere. Ethanol (300 mL) and ether (300 mL) were then added to the brown mixture at 0°C before filtering the solution. The brown residue was poured in 50 mL of concentrated HCl and 200 mL of ethanol. After 20 hours of stirring the solution was filtered and the solid was washed using ethanol and ether, giving 5.51 g of a light grey product in a 75 % yield. NMR ^{1}H (300 MHz, D_2O): δ 3.42 (s, 12H, CH_2).

1,4,7-Triazacyclononane (TACN). 1,4,7-Triazacyclononane · 3 HCl (5.51 g, 0.023 mol) was dissolved in 100 mL of toluene before adding 2.01 g of NaOH in 20 mL of water. The mixture was then heated to 100 °C and the water extracted using a Dean-Stark apparatus. The solution was then filtered and the solvent carefully evaporated to give 1.31 g of a yellow volatile oil in a 51 % yield. NMR ^{1}H (300 MHz, D_2O): δ 2.80 (s, 12H, CH_2).
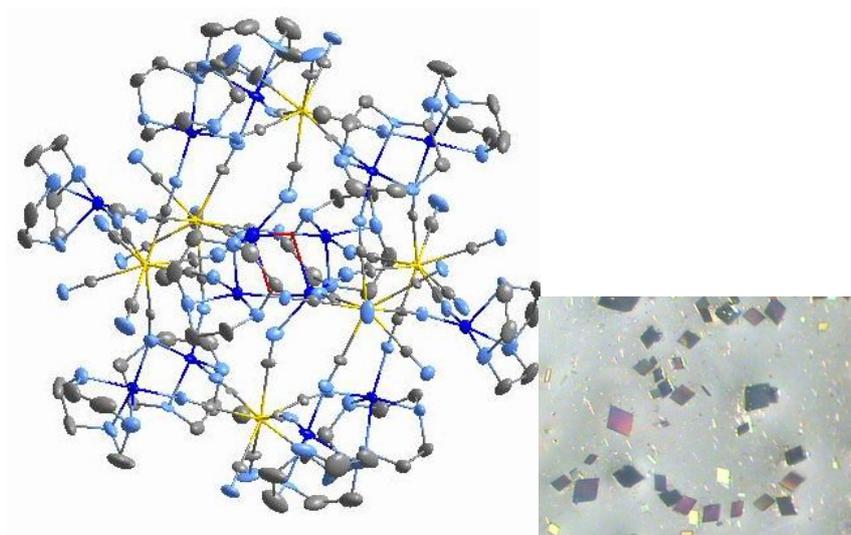
2. X-Ray Crystallography

Figure S3: Ortep representation of the X-ray crystal structure of **1** (thermal ellipsoids set at 50 % probability level)
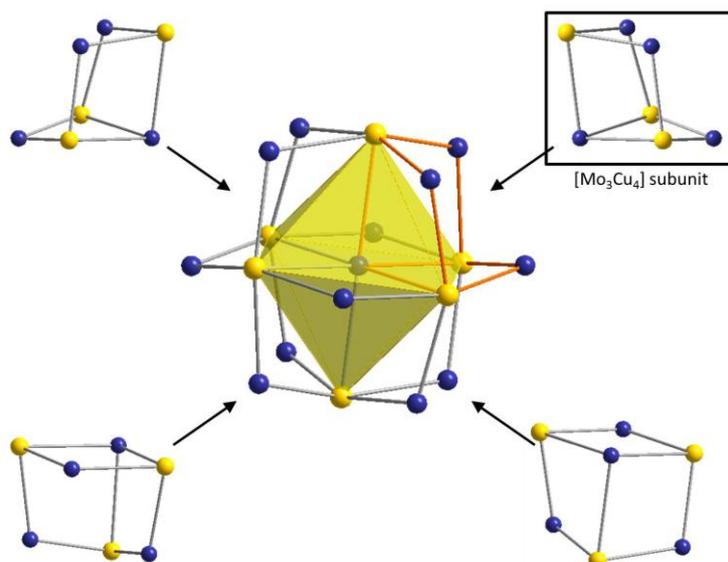

Figure S4: Formation of **1** viewed as the association of 4 [Mo$_3$Cu$_4$] subunits

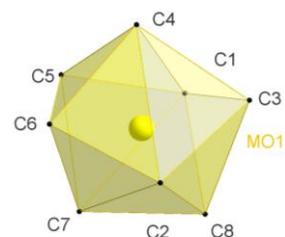| [Mo^{IV}(CN)$_8$]	(APBC-8) D_{4d}	(DD-8) D_{2d}
Mo	1.79748	0.36158

Table S1: Shape analysis of the coordination polyhedra of Molybdenum atoms for **1**

Crystal data and structure refinement for [Mo$_6$Cu$_{14}$-tacn](1)

Empirical formula	C133.60 H338 Cl2 Cu14 Mo6 N90.80 O80.80
Formula weight	6046.22
Temperature	200(2) K
Wavelength	0.71073 Å
Crystal system	Triclinic
Space group	P -1
Unit cell dimensions	a = 19.1825(10) Å α= 76.569(3)°.
	b = 19.3041(10) Å β= 75.823(3)°.
	c = 19.3498(10) Å γ = 75.935(3)°.
Volume	6624.1(6) Å^3
Z	1
Density (calculated)	1.516 Mg/m^3
Absorption coefficient	1.480 mm^{-1}
F(000)	3114
Crystal size	0.12 x 0.09 x 0.08 mm^3
Theta range for data collection	1.405 to 27.720°.
Index ranges	-25<=h<=24, -21<=k<=25, -24<=l<=25
Reflections collected	75398
Independent reflections	30033 [R(int) = 0.0536]
Completeness to theta = 25.242°	98.7 %
Absorption correction	Semi-empirical from equivalents
Max. and min. transmission	0.746 and 0.615
Refinement method	Full-matrix least-squares on F^2
Data / restraints / parameters	30033 / 90 / 1522
Goodness-of-fit on F^2	1.111
Final R indices [I>2sigma(I)]	R1 = 0.1048, wR2 = 0.2529
R indices (all data)	R1 = 0.1388, wR2 = 0.2688
Extinction coefficient	n/a
Largest diff. peak and hole	4.840 and -1.653 e.Å^{-3}

Single Crystal X-Ray Structure of [Mo₃Cu₄-Me₃tacn](2)

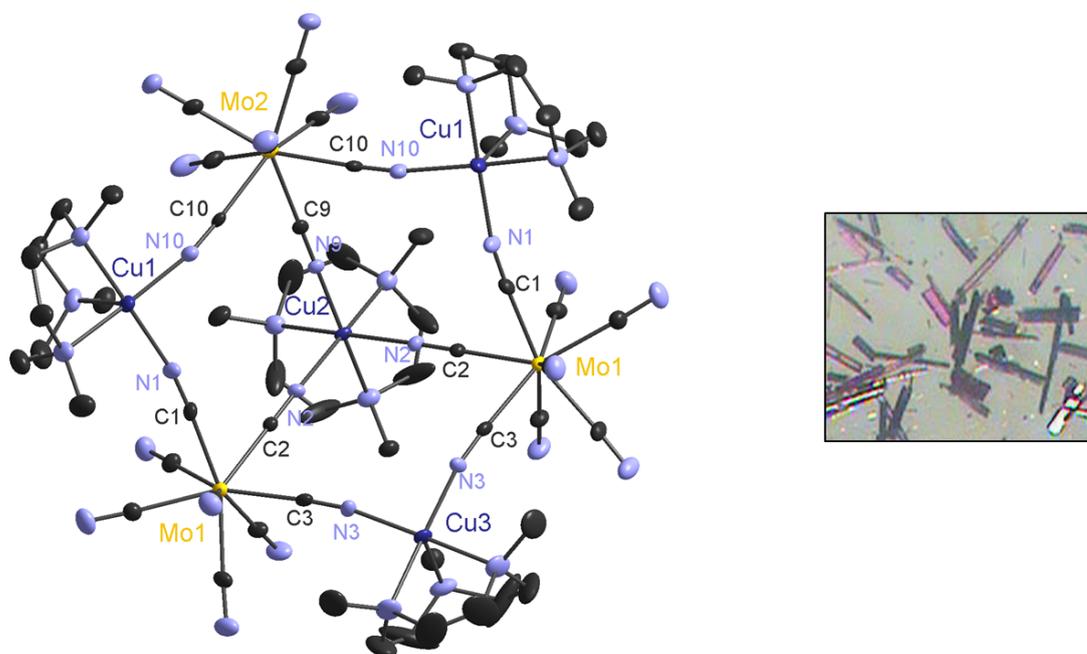**Single Crystal X-Ray Structure of [Mo$_3$Cu$_4$-Me$_3$tacn](2)**

Figure S5:*Ortep representation of the X-ray crystal structure of **2***
(thermal ellipsoids set at the 30 % probability level)

Interatomic distances (Å)		Angles (°)	
Mo1-C	2.1381(78)-2.1735(98)	Mo1-C-N (bridge)	176.366(652)-176.690(671)
Mo2-C	2.1463(133)-2.1766(102)	Mo1-C-N (free)	177.452(754)-178.190(634)
C-N (free)	1.1322(144)-1.1550(128)	Mo2-C-N (bridge)	176.663(700)-177.172(839)
C-N (bridge)	1.1362(97)-1.1565(133)	Mo2-C-N (free)	177.608(923)-177.750(788)
Cu1-N (CN bridge)	1.9600(69)-1.982(8)	C-N-Cu1	167.818(658)-168.528(728)
Cu2-N (CN bridge)	2.0381(95)-2.1180(62)	C-N-Cu2	173.117(593)-177.553(858)
Cu3-N (CN bridge)	1.9655(62)	C-N-Cu3	168.929(600)
Cu1-N (ligand)	2.0512(69)-2.1818(77)	N-Cu-N (cycle Mo₃Cu₃)	90.932(246)-91.105(306)
Cu2-N (ligand)	2.1205(101)-2.1911(80)	C-Mo-C (cycle Mo₃Cu₃)	105.942(288)-106.873(298)
Cu3-N (ligand)	2.0587(97)-2.1670(134)	C1-Mo1-C2, C3-Mo1-C2, C10-Mo2-C9	73.384(187), 74.107(297), 73.457(181)
Mo1---Cu1	5.2080(12)		
Mo1---Cu2	5.4080(9)		
Mo1---Cu3	5.2291(10)		
Mo2---Cu1	5.2366(12)		
Mo2---Cu2	5.3531(14)		
Mo1---Mo2	8.5332(100)		
Cu1---Cu2	6.7247(13)		
Cu1---Cu3	8.9395(15)		
Cu2---Cu3	6.7770(16)		

Table S2: *Selected interatomic distances and angles for **2***

[$Mo^{IV}(CN)_8$]	(APBC-8) D_{4d}	(DD-8) D_{2D}
Mo1	0.32057	1.84374
Mo2	0.40650	2.09128

Table S3: *Shape analysis of the coordination polyhedra of Molybdenum atoms for* **2**
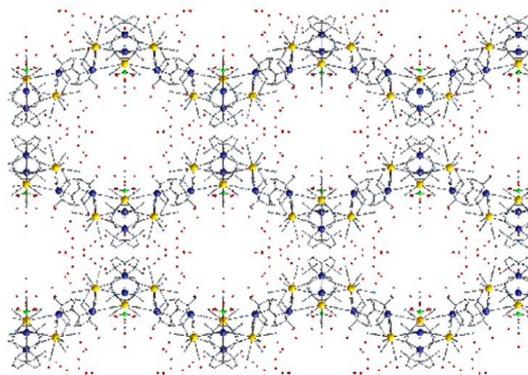

Figure S6: X-ray crystal structure of **2** exhibiting the channel alignment along the *b* axis

Crystal data and structure refinement for [Mo₃Cu₄-Me₃tacn](2)

Empirical formula	C120 H168 Cu9 Mo6 N80 O70
Formula weight	4998.83
Temperature	200(1) K
Wavelength	0.71073 Å
Crystal system	Orthorhombic
Space group	P n n m
Unit cell dimensions	a = 33.5532(15) Å $\quad\quad\quad$ α = 90°.
	b = 16.9349(7) Å $\quad\quad\quad$ β = 90°.
	c = 27.2581(11) Å $\quad\quad\quad$ γ = 90°.
Volume	15488.6(11) Å^3
Z	2
Density (calculated)	1.072 Mg/m^3
Absorption coefficient	0.903 mm^{-1}
F(000)	5042
Crystal size	0.3 x 0.15 x 0.1 mm^3
Theta range for data collection	0.962 to 28.700°.
Index ranges	-45<=h<=45, -22<=k<=22, -36<=l<=36
Reflections collected	111283
Independent reflections	20401 [R(int) = 0.0518]
Completeness to theta = 25.242°	100.0 %
Absorption correction	Semi-empirical from equivalents
Max. and min. transmission	0.7458 and 0.6722
Refinement method	Full-matrix least-squares on F^2
Data / restraints / parameters	20401 / 0 / 710
Goodness-of-fit on F^2	1.180
Final R indices [I>2sigma(I)]	R1 = 0.1128, wR2 = 0.3031
R indices (all data)	R1 = 0.1425, wR2 = 0.3242
Largest diff. peak and hole	2.047 and -1.957 e.Å^{-3}

3. **Magnetic Properties for [Mo$_6$Cu$_{14}$-tacn] (1)**

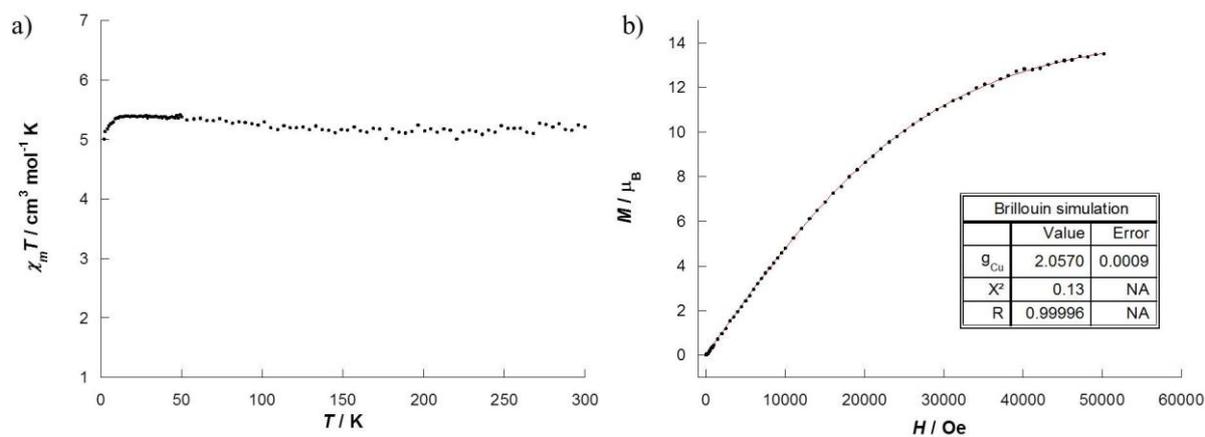| Brillouin simulation		
	Value	Error
g$_{Cu}$	2.0570	0.0009
X²	0.13	NA
R	0.99996	NA

Figure S7:*a) Variation of χ$_m$T vs. T (H=1000G) for **1**;*
b) M vs. H at 2K,Brillouin simulation
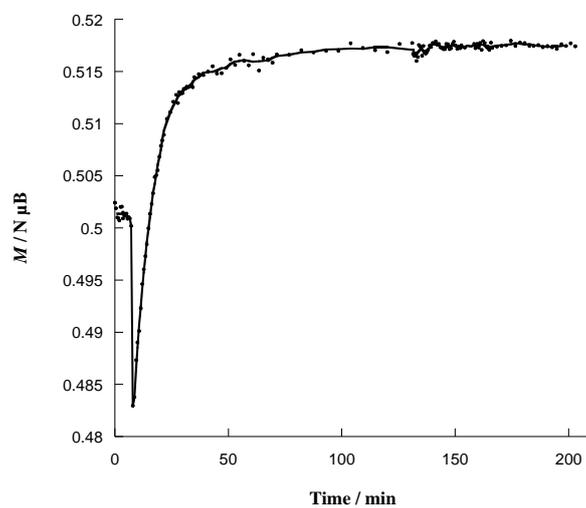
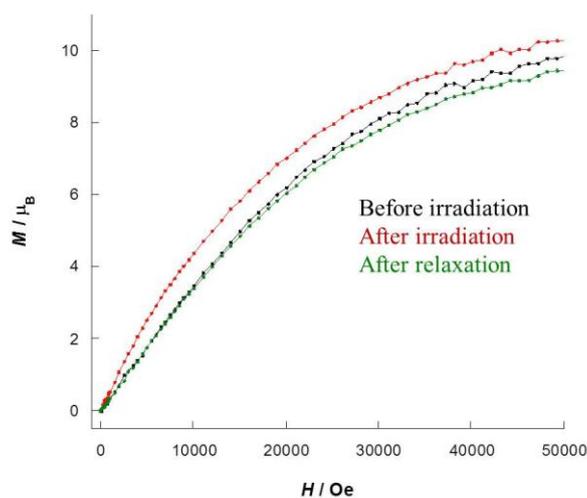***Figure S8:****Magnetization recorded as a function of irradiation time for **1***

Before irradiation
After irradiation
After relaxation

Figure S9*: Field sweep of **1**before (black),after (red) irradiation,*
and after relaxation (green)

8

4. Magnetic properties for [Mo$_3$Cu$_4$-Me$_3$tacn](2)

Investigation of the photomagnetic properties of complex **2** shows at room temperature a χ_mT value of 2.83 cm^3.mol^{-1}.K spectroscopies (**see SI-FigureS12**), in agreement with the theoretical values of 2.36 corresponding to at least six independent copper atoms (Cu^{II}, d^9, S = 1/2, *g* = 2.05), including the suspected copper atoms included in holes of the MOF structure, as confirmed by elemental analysis and EPR. Field sweep plot of **2** (**ESI-Figure S6**) shows a maximum value of 6.15 µB at 90 kOe in agreement with the presence of six Cu^{II} atoms (g_{Cu} = 2.05).
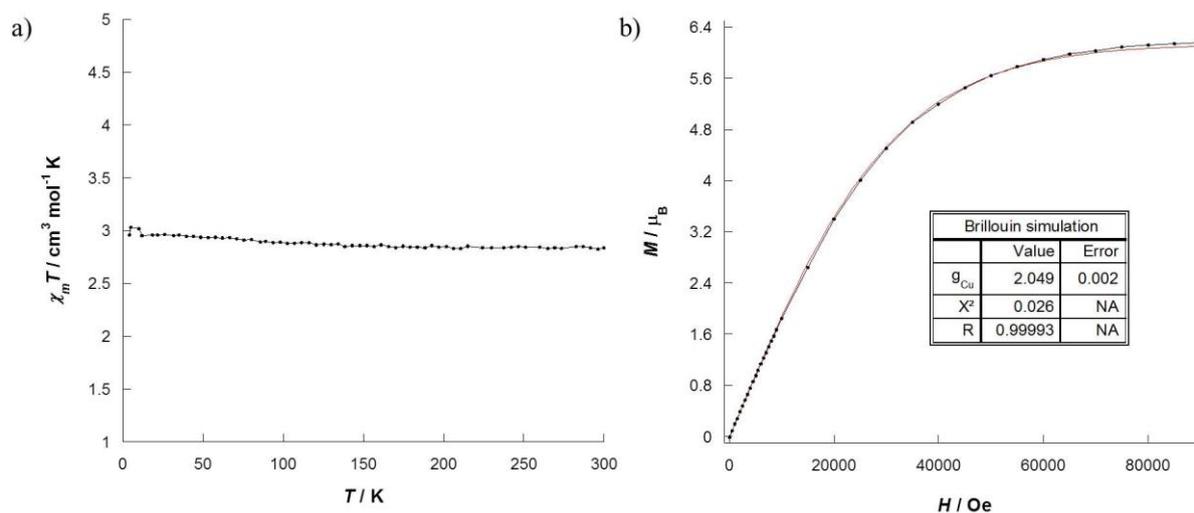

Figure S10:*a) Variation of χ_mT vs. T (H=1000G) for **2**; b) M vs. H at 2.2K for **2**, Brillouin simulation*
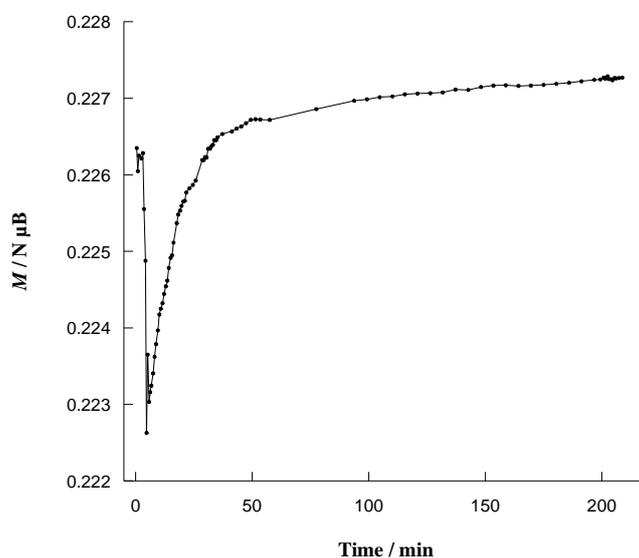

Figure S11:*Magnetization recorded as a function of irradiation time for **2**. The decrease of magnetization observed when the laser beam is switched on is attributed to a small increase of temperature of the sample.*
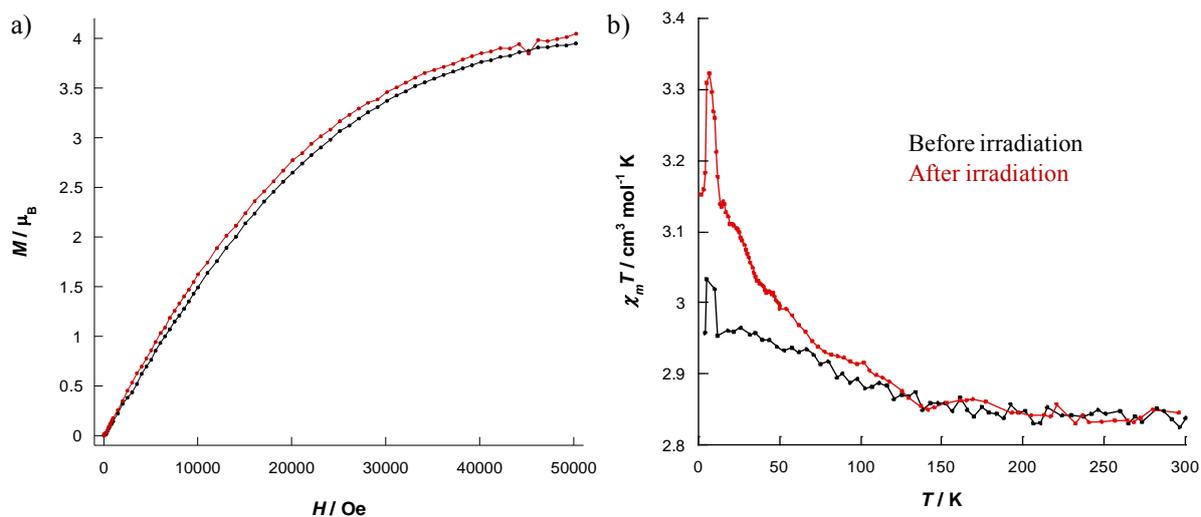
Figure S12*: a) Field sweep before (black) and after (red) irradiation for **2***
b) Variation of $\chi_m T$ vs. Tbefore and after irradiation

5. EPR spectroscopy studies

Upon irradiation the signal immediately decreased, reflecting the coupling of the Cu^{II} ions. Complex **2** exhibited an almost complete quenching of the Cu^{II} signal less important thant what is observed for 1. This difference of behavior can be expected from the presence of the residual non-photoactive Cu^{II} ions located in the channels formed in crystals of **2**.
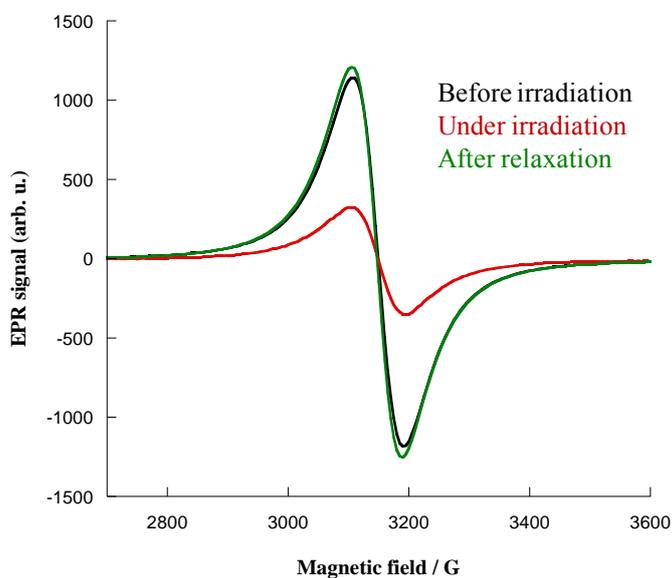

Figure S3: EPR spectra for **2** before (black) and under (red) irradiation,
and after relaxation (green)